

RESEARCH

Open Access



Secreted protein NFA47630 from *Nocardia farcinica* IFM10152 induces immunoprotective effects in mice

Lichao Han^{1,2}, Xingzhao Ji³, Shihong Fan⁴, Jirao Shen², Bin Liang³ and Zhenjun Li^{2*}

Abstract

Purpose *Nocardia* is emerging as a common and easily neglected cause of both healthcare- and occupation-associated infections worldwide, however, human vaccines for *Nocardia* prevention are not yet available. In this study, we aimed to evaluate the immunoprotective effect of the NFA47630 protein, a secreted protein abundant in the *N. farcinica* IFM10152 supernatant.

Methods Conservation and characteristics of *nfa47630* were analyzed by PCR and bioinformatics. Then recombinant NFA47630 protein was cloned, expressed and purified for further antigenicity analysis. Subsequently, the ability to activate innate immunity was evaluated by examining the phosphorylation status of the MAPK signaling pathway and cytokine levels. Finally, the protective effect was evaluated on rNFA47630-immunized mice.

Results *nfa47630* was conserved in *N. farcinica* strains with good antigenicity. The rNFA47630 protein was expressed under the optimal conditions of 0.2 mM IPTG, 28 °C, and it can be recognized by anti-*N. farcinica* and anti-*N. cyriacigeorgica* sera, but not anti-*N. asteroides*, anti-*N. brasiliensis*, anti-*N. nova* and anti-*Mycobacterium bovis* sera. It can upregulate the phosphorylation status of ERK, JNK, P38 and the cytokine levels of TNF- α , IL-10, IL-12, and IFN- γ . In addition, mice immunized with rNFA47630 protein exhibited higher antibody titers, greater bacterial clearance ability, milder organ infection, and higher survival rates than PBS-immunized mice.

Conclusions Our data demonstrate that NFA47630 is a potential vaccine candidate for defending against *N. farcinica* infection.

Keywords *Nocardia farcinica*, NFA47630, Immunoprotective effects, Vaccine

Introduction

Nocardia species are a group of gram-positive bacilli belonging to the *Nocardia* genus, *Nocardiaceae* family, *Corynebacteriales* order and *Actinobacteria* phylum [1]. It encompasses more than 120 recognized species with valid names (<https://www.bacterio.net/genus/nocardia>) [2], and the primary implicated human and animal pathogens include *N. farcinica*, *N. cyriacigeorgica*, *N. brasiliensis* and *N. asteroides* [3].

The occurrence of nocardiosis has been reported in immunocompromised [4, 5] and immunocompetent [6] individuals in many countries, especially in America, India, Mexico, Japan, Spain, France, Australia,

*Correspondence:

Zhenjun Li
lizhenjun@icdc.cn

¹ Department of Traditional Chinese Medicine, Shandong Provincial Hospital Affiliated to Shandong First Medical University, Jinan, China
² Chinese Center for Disease Control and Prevention, State Key Laboratory of Infectious Disease Prevention and Control, National Institute for Communicable Disease Control and Prevention, 155 Changbai Road Changping District, 102206 Beijing, People's Republic of China

³ Department of Pulmonary and Critical Care Medicine, Shandong Provincial Hospital Affiliated to Shandong First Medical University, Jinan, China

⁴ Sericulture and Apiculture Research Institute, Yunnan Academy of Agricultural Science, Mengzi, Yunnan, China



© The Author(s) 2024. **Open Access** This article is licensed under a Creative Commons Attribution-NonCommercial-NoDerivatives 4.0 International License, which permits any non-commercial use, sharing, distribution and reproduction in any medium or format, as long as you give appropriate credit to the original author(s) and the source, provide a link to the Creative Commons licence, and indicate if you modified the licensed material. You do not have permission under this licence to share adapted material derived from this article or parts of it. The images or other third party material in this article are included in the article's Creative Commons licence, unless indicated otherwise in a credit line to the material. If material is not included in the article's Creative Commons licence and your intended use is not permitted by statutory regulation or exceeds the permitted use, you will need to obtain permission directly from the copyright holder. To view a copy of this licence, visit <http://creativecommons.org/licenses/by-nc-nd/4.0/>.

Brazil, China and Thailand [7]. As an opportunist pathogen, *Nocardia* is capable of producing serious infections in appropriate hosts. Pulmonary infection is the most common clinical presentation because inhalation of airborne spores is the primary transmission route of bacterial exposure [8, 9]. Primary cutaneous and subcutaneous nocardiosis can result from traumatic injury that involves soil contamination, especially in gardeners and farmers [10]. Central nervous system (CNS) nocardiosis usually occurs in patients with one or more brain abscesses, accompanied by symptoms of headache, vomiting and depressed consciousness [6, 11]. Other common sites of nocardial dissemination include the eye, pericardium, mediastinum, liver, spleen, and thyroid [3, 8]. Disseminated nocardiosis often involves lungs and CNS, causing unsatisfactory prognosis. One-year mortality rates are estimated to be as high as 16–85% depending on study populations [12].

One of the important reasons for the poor prognosis of disseminated nocardiosis is that the optimal antimicrobial treatment recommendations for nocardiosis have not been firmly established. Given that *Nocardia* species display variable in vitro antimicrobial susceptibility patterns [10], nocardiosis management must be individualized. The combination of multiple agents is always performed in patients with severe nocardiosis, such as INF- γ [12]. Because antibiotic therapies always extend for months or even years, resistance to first-line antibiotics [13, 14], such as trimethoprim-sulfamethoxazole (TMP-SMX) [15], rifampicin [16], and aminoglycoside [17], have emerged in several cases. The high mortality rate of disseminated nocardiosis and the emergence of drug-resistant strains have led to an in-depth study of prevention options for *Nocardia* infection from immunological insights. However, few studies have focused on the immunoprotective proteins of *Nocardia* thus far.

A previous study in our laboratory identified over 500 secreted proteins in *N. farcinica* IFM10152 supernatant by LC-MS/MS, and NFA47630 protein is one of the proteins with high content [18]. In this study, we first performed a conservative and bioinformatic analysis of the NFA47630 protein. Then, we cloned and expressed recombinant NFA47630 protein in *Escherichia coli* BL21, and its antigenicity and ability to activate the innate signaling pathway were subsequently determined. Finally, by analyzing its immunoprotective efficacy in rNFA47630-immunized mice, we concluded that the rNFA47630 protein can induce functional antibody responses in mice and holds great promise as a potential vaccine candidate.

Materials and methods

Mice and ethics statement

Six- to eight-week-old BALB/c female mice were procured from SPF Biotechnology Co., Ltd. (Beijing, China) and bred under specific pathogen-free conditions following standard and approved protocols. All animal procedures were conducted in compliance with the Ethics Review Committee of the National Institute for Communicable Disease Control and Prevention at the Chinese Center for Disease Control and Prevention (protocol code 2020–018). All efforts were made to minimize suffering.

Bacterial strains and culture conditions

N. farcinica IFM10152 strain was procured from the German Resource Centre for Biological Materials. Twenty-three *N. farcinica* isolates were randomly selected from our laboratory and cultured in BHI broth (Oxoid Ltd, UK) at 37 °C. *Escherichia coli* BL21(DE3) was procured from TransGen Biotech and cultured in LB medium containing kanamycin (50 μ g/ml). All strains were cultured to exponential phase before experiments.

Conservative and bioinformatic analysis

For conservative analysis, the *nfa47630* sequence was matched with *N. farcinica* sequences by NCBI Nucleotide Blast. To further verify its conservation in clinical strains, DNA was extracted from *N. farcinica* IFM10152 and 23 isolated *N. farcinica* strains (Table S1) using the Wizard Genomic DNA Purification Kit (Promega, USA), and PCR was performed using *nfa47630* specific primers: forward 5'-ATCTGAATTCATGCCGACCGCAGTAG-3' and reverse 5'-ATGTAAGCTTTCAGGCGACGGTGAAG-3'. PCR products were then detected by 2% agarose gel electrophoresis. The bioinformatic analysis of NFA47630 was performed by searching (I) subcellular localization using PSORTb (<https://www.psорт.org/psорт/>) [19], (II) signal peptide using UniProt (<https://www.uniprot.org/>) [20], (III) transmembrane helices using HMMTOP (<http://www.enzīm.hu/hmmtop/>) [21], and (IV) antigenic propensity using Protein Variability Server (<http://imed.med.ucm.es/PVS/>) [22].

Expression and purification of recombinant NFA47630 proteins

For preparation of recombinant proteins, plasmids were cloned into the pET-30a(+) expression vector by digestion with *EcoR* I and *Hind* III and transformed into *Escherichia coli* BL21(DE3). Recombinant *E. coli* BL21 cells were selected and grown in LB medium containing 50 μ g/ml kanamycin at 37 °C for 6 h until the OD₆₀₀ reached 0.8. Then, protein expression was induced by the addition of 0.2, 0.5 and 1 mM IPTG to the bacterial

culture for 4 h at 28 and 37 °C. After the bacterial suspension was sonicated with protease inhibitor, the pellet and culture supernatant were obtained by centrifugation at 12,000 rpm/min for 20 min at 4 °C, and all protein preparations were analyzed by SDS–PAGE and quick blue staining. The recombinant NFA47630 (rNFA47630) protein was then purified using the His-Bind purification kit (Novagen, Germany). After the collected protein was eluted by a Ni–NTA column with elution buffer, nonspecific proteins were removed by washing with 20, 40, 60, 100, and 250 mM imidazole buffer. All eluted fractions were collected and analyzed by SDS–PAGE and quick blue staining. Purified protein was then concentrated with a 10-kDa centrifugal filter device (Millipore, MA), and endotoxin was further removed using a ToxinEraser endotoxin removal kit (GenScript, China) according to the manufacturer's guidelines. The protein was stored at -80 °C after concentration determination by a bicinchoninic acid (BCA) assay.

Antigenicity determination by western blot

Total rNFA47630 proteins were separated by SDS–PAGE (5–12%) and transferred onto 0.45 µm polyvinylidene fluoride (PVDF; Merck, Germany) membranes. The membranes were then blocked with 5% skim milk diluted in TBS containing 0.05% Tween (TBST) for 2 h at room temperature. Mouse antisera (stored in our laboratory) included *N. farcinica*, *N. asteroides*, *N. cyriaciageorgoca*, *N. brasiliensis*, or *Mycobacterium bovis*, and horseradish peroxidase (HRP)-conjugated monoclonal anti-pentahistidine (His) antibody (New England Biolabs Inc., USA) was diluted (1:2,000) in TBST containing 2% skim milk and incubated overnight at 4 °C. The membranes were then washed with TBST three times and incubated in an HRP-conjugated goat anti-mouse IgG (1:4000; Southern Biotech, USA) secondary antibody for 1 h at room temperature. After three washes with TBST, the bands were visualized using Amersham® Hyperfilm® ECL™ and MP Autoradiography Films (GE Healthcare).

Cell culture

The mouse macrophage cell line RAW264.7 was procured from the National Infrastructure of Cell Line Resource (Beijing, China) and cultured in high-glucose DMEM (Gibco, NY, USA) supplemented with 10% FBS at 37 °C. In each experiment, cells from passages 5 to 15 were counted before seeding in the plate.

MAPK signaling pathway analysis

For MAPK signaling pathway analysis, RAW264.7 cells were seeded in 6-well microplates at a density of 8×10^5 cells per well for 16–18 h and then stimulated with 2, 4 or 8 µg/mL rNFA47630 protein. In order to exclude

residual LPS interference, rNFA47630 preparation was pretreated with 100 µg/ml polymyxin B (PmB, a specific inhibitor for LPS, INALCO, USA) at 37 °C for 2 h [23]. Additionally, 100 ng/mL LPS (with or without 100 µg/mL PmB) was added to the cell plate as positive control. At indicated time points, whole-cell extracts were harvested using RIPA lysis buffer (strong) (CW BIO, Beijing, China) containing protease and phosphatase inhibitor cocktail for Western blot analysis. Equal amounts of protein were separated by SDS–PAGE and transferred to PVDF membranes as described before. Primary antibodies against p-ERK1/2 (1:1000, CST, USA), p-JNK (1:1000, CST, USA), p-P38 (1:1000, CST, USA), and β-actin (1:4000, CST, USA) were diluted in TBST containing 2% skim milk. HRP-conjugated goat anti-rabbit IgG (1:1000, Beyotime, China) or HRP-conjugated goat anti-mouse IgG (1:4000, ZSGB-BIO, China) was used as the secondary antibody.

Cytokine measurements

To measure cytokines in rNFA47630-stimulated RAW264.7 cells, cells were seeded in 24-well culture microplates at a density of 2×10^5 /well and 2 µg of rNFA47630 was added for 6, 18 and 24 h. Similarly, we set up rNFA47630 + PmB and LPS (with or without PmB) groups to test residual LPS effects. To block MAPK signaling, cells were pretreated for 1 h with inhibitors of 20 µM ERK (PD 98059, Sigma, USA), 20 µM JNK (SP 600125, Sigma, USA) or 20 µM p38 (SB 203580, Sigma, USA) prior to rNFA47630 protein exposure. Then, culture supernatants were harvested at the indicated times, and the cytokine concentrations were determined by TNF-α, IL-10, IL-12 and IFNγ ELISA kits (BD OptEIA™, USA) according to the manufacturer's instructions.

Mouse immunization

Female mice were randomly divided into rNFA47630 and PBS groups and immunized by intramuscular injection of 100 µl recombinant protein-aluminum hydroxide adjuvant mixture (10 µg of rNFA47630 per mouse) or equivalent PBS-aluminum hydroxide adjuvant mixture three times every 2 weeks. Whole blood (with the addition of the anticoagulant heparin) and sera in rNFA47630-immunized (n=6) and PBS-immunized mice (n=6) were collected 7 days after the last immunization, and rNFA47630-specific IgG, IgG1, IgG2a and IgG2b (Abcam, UK) antibodies were determined by ELISA. To confirm antibody production during infection, rNFA47630 protein was separated by SDS–PAGE and transferred to PVDF membranes as described before. Anti-rNFA47630 sera (1:2000) were used as the primary antibodies, followed by a secondary antibody (HRP-conjugated goat anti-mouse IgG).

Whole blood and neutrophil killing assay

Equal whole blood (with the addition of the anticoagulant heparin) from rNFA47630- and PBS-immunized mice was collected and immediately mixed with a 1×10^6 CFU *N. farcinica* suspension in a 37 °C incubator for 2 h. Then, serial dilutions of mixtures were plated on BHI agar plates for CFU count.

Mice were then sacrificed by cervical dislocation, and femurs and tibias in PBS-immunized mice were dissected and flushed out with HBSS (Solarbio, China) for bone marrow cell isolation. Subsequently, marrow suspensions were centrifuged at $500 \times g$ and 4 °C for 10 min, and the pellets were resuspended with 45% Percoll and overlaid onto Percoll gradient layers (81%, 62%, 55%, and 50%). After centrifugation at $500 \times g$ for 30 min, cells were collected from the 81%/62% interface, and red blood cells were depleted using RBC lysis buffer (BD OptEIA™, CA, USA). Bone marrow neutrophils were then counted and incubated in a 24-well microplate at a density of 2×10^5 cells per well with RPMI 1640 medium supplemented with 10% FBS. After 24 h of stimulation with 2 µg of rNFA47630, *N. farcinica* suspension was added to each well at a ratio of 10:1 for 2 h of incubation, and serial dilutions of whole cell lysates were then plated on BHI agar plates for bacterial survival determination.

Spleen cell isolation

Spleens in PBS-immunized mice were dissected and transferred into a 40 µm cell strainer placed within a 50 ml tube, then mashed gently with a 5 ml syringe plunger and washed repeatedly with 1×HBSS. After centrifugation at $500 \times g$ for 10 min twice and depleting red blood cells using RBC lysis buffer, spleen cells were incubated in a 24-well microplate with RPMI 1640 medium supplemented with 10% FBS and stimulated with 2 µg of rNFA47630. Supernatants were collected after 1, 2, and 3 days of incubation, and the cytokine concentrations of IFN-γ and IL-4 were determined by ELISA kits as described above.

Mouse challenge

Ten days after the last immunization, mice in the rNFA47630 (n=10) and PBS (n=10) groups received 50 µl of *N. farcinica* (1×10^7 CFU) suspension through intranasal inoculation. Loss of weight and elevated body temperature were quantified immediately prior to infection and 24 h postinfection as previously described. Pulmonary bronchoalveolar lavage fluid (BALF) was obtained through 3 successive lavages of the bronchi with ice-cold PBS for lactate dehydrogenase (LDH) assessment using the LDH-Glo™ Cytotoxicity Assay (Promega, USA) procedures. Whole lungs were collected and homogenized and then plated on BHI agar plates by serial

dilutions. Bacterial counts were enumerated after 48 h in a 37 °C incubator. Lung homogenate was then centrifuged to obtain the supernatant samples, and the concentrations of TNF-α, IL-10, IL-12, and IFN-γ were determined by ELISA as described above.

For survival rate analysis, each mice in the rNFA47630 (n=10) and PBS (n=10) groups were challenged by intraperitoneal injection of 100 µl (1×10^9 CFU) bacterial suspension, and mouse survival was monitored daily for a 10-day period. To assess the severity of pathological damage, surviving mice were sacrificed by cervical dislocation. Lungs, liver and brain tissues were collected and fixed in 4% paraformaldehyde, embedded in paraffin and sectioned. Subsequently, the deparaffinized tissue sections were stained with hematoxylin and eosin (H&E). Stained sections were observed using a biological microscope (Nikon, Eclipse Ci-L, Japan), and images were randomly captured under high-power fields (20× magnification).

Statistical analysis

All statistical analyses were performed using GraphPad Prism 9.0.0. Statistical differences were analyzed using ordinary one-way analysis of variance (ANOVA) with Tukey's multiple comparisons. Survival rates were analyzed by Kaplan–Meier and log rank test. For all experiments, values of differences $p \leq 0.05$ were considered statistically significant.

Results

The NFA47630 protein was conserved in *N. farcinica* strains with potential antigenicity

NFA47630 is an extracellular protein with 237 amino acids. Based on Nucleotide-Blast analysis, we obtained 99.36–100% similarity for the *nfa47630* sequence among all 42 *N. farcinica* strains uploaded in the NCBI database. We then examined the positivity of the *nfa47630* gene in clinical strains by PCR. The obtained results (Fig. 1) showed that all 23 clinical strains contained the *nfa47630* gene fragment with the same size as in the *N. farcinica* IFM10152 strain, which indicates that it is conserved in *N. farcinica* species. PSORTb analysis revealed that the uncharacterized protein NFA47630 was located extracellularly. UniProt and HMMTOP predicted that it possesses one signal peptide with 29 amino acids (1 aa~29 aa) and two transmembrane helices (46 aa~69 aa, 90–109 aa). Protein Variability Server predicted that it possesses eleven possible antigenic determinants (aa4~aa10, aa21~aa82, aa90~aa120, aa136~aa144, aa154~aa175, aa179~aa186, aa191~aa20, aa211~aa217, aa227~aa235, aa240~aa248, aa258~aa270) with an average antigenic propensity index of 1.0416, indicating its potential strong antigenicity.

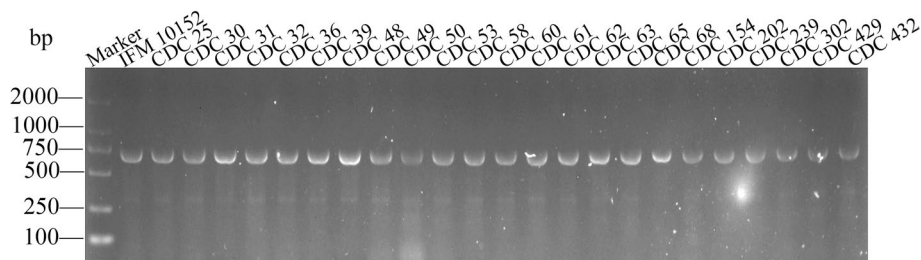


Fig. 1 *N. farcinica* clinical strains share the *nfa47630* gene fragment with the same size. DNA was extracted from *N. farcinica* IFM 10152 and 23 isolated *N. farcinica* strains, followed by PCR using *nfa47630* specific primers. PCR products were then detected by 2% agarose gel electrophoresis

rNFA47630 protein was expressed and purified under optimal conditions

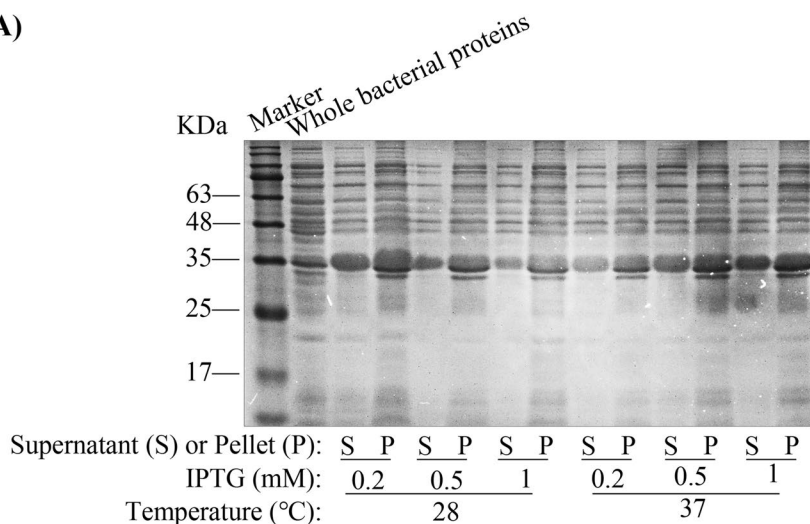
DNA electrophoresis showed a single band with the expected size, and nucleotide sequencing analysis confirmed that the pET30a-*nfa47630* recombinant expression vector was constructed correctly. As shown in Fig. 2A, SDS-PAGE analysis indicated that after cells were induced with 0.2 mM IPTG for 4 h at 28 °C, NFA47630 protein in the supernatant exhibited increased expression. Purified rNFA47630 protein

presented as a single band (Fig. 2B) at a concentration of 800 µg/ml.

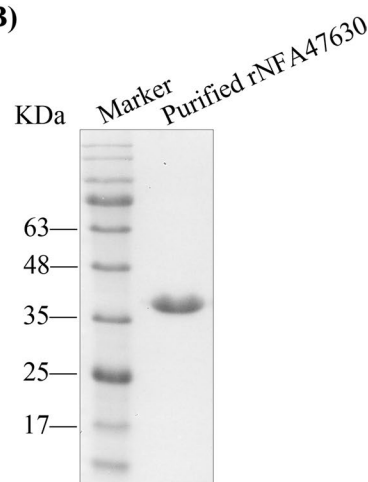
The rNFA47630 protein can be recognized by anti-*N. farcinica* and anti-*N. cyriaciageorgica* sera

To validate the potential antigenicity of rNFA47630, western blotting was conducted to detect rNFA47630-specific antibodies from the sera of *N. farcinica*-infected mice. The obtained results (Fig. 2C) suggested that rNFA47630 can be detected with anti-His antibody and sera from

(A)



(B)



(C)

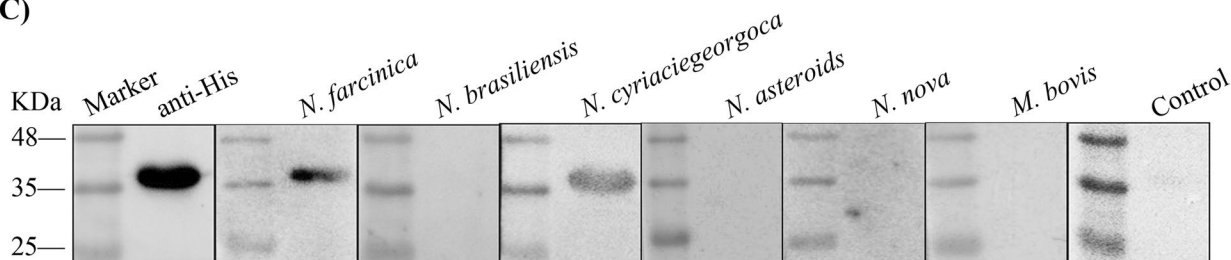


Fig. 2 Expression, purification and antigenicity analysis of the rNFA47630 protein. **A** Screening optimal expression conditions of location, IPTG concentration, and temperature. **B** Purified rNFA47630 protein. **C** Reactivity of the rNFA47630 protein with antisera from mice infected with anti-His, *Nocardia* species or *M. bovis*

N. farcinica-infected mice but not from the controls. To assess the specificity of rNFA47630, we used antisera from mice infected with other *Nocardia* species and *M. bovis*. The obtained results revealed that the rNFA47630 protein can be recognized by anti-*N. cyriacigeorgica*, but not anti-*N. asteroides*, anti-*N. brasiliensis*, anti-*N. nova* and *M. bovis* sera, which indicates that the rNFA47630 protein can cross-react with some *Nocardia* species but possesses interspecies specificity.

rNFA47630 activated the MAPK signaling pathway in RAW264.7 cells

Previous research demonstrated that *Nocardia* not only invades epithelial cells but also survives in macrophages [24–26]. To investigate whether the rNFA47630 protein regulates the MAPK signaling pathway, we examined the phosphorylation statuses of ERK1/2, JNK and p38 in RAW264.7 cells at 30 min post-stimulation. The results showed increased phosphorylation levels of p-JNK, p-JNK, and p-p38 in rNFA47630, rNFA47630+PmB and LPS-stimulated groups compared with control group, but not in LPS+PmB group (Fig. 3A), which indicated rNFA47630 protein capable of activating MAPK signaling pathways independently of residual LPS. Subsequently, RAW264.7 cells were stimulated with rNFA47630 protein (2 µg/mL for 30, 60, 120 min, or 2, 4 or 8 µg/mL for 30 min) for elucidating the relationship between phosphorylation statuses of MAPK signaling pathway and the concentration of rNFA47630 protein, stimulation time. The obtained results showed that stimulation with 2 µg/mL rNFA47630 for 30 min resulted in evident phosphorylation of ERK1/2, JNK and p38, and the phosphorylation status of JNK and p38 gradually decreased to baseline after 2 h of stimulation (Fig. 3B). In addition, we found that the phosphorylation levels of JNK and p38 gradually increased, while ERK1/2 gradually decreased with increasing rNFA47630 protein concentration (Fig. 3C), further indicating that the rNFA47630 protein plays a key role in activating the MAPK pathways in RAW264.7 cells in a time- and dose-dependent manner.

rNFA47630-induced cytokine secretion depended on the MAPK pathways

To confirm the ability of rNFA47630 protein to induce cytokine expression, RAW264.7 macrophages were stimulated with rNFA47630 (with or without PmB) or LPS (with or without PmB) for indicated time point. The results showed that the concentrations of TNF-α, IL-10, IL-12, and IFN-γ increased over time and reached higher levels at 24 h of stimulation in rNFA47630 group (Fig. 3D). Furthermore, cytokine levels remained high even after the addition of PmB, suggesting that the rNFA47630 protein was able to stimulate cytokine

secretion from RAW264.7 cells, as we confirmed that 100 µg/mL PmB could completely counteract the effect of LPS (Fig. 3D). To further elucidate the roles of ERK1/2, JNK and p38 in rNFA47630-induced cytokine production, RAW264.7 macrophages were pretreated with specific molecular signaling inhibitors for 1 h followed by rNFA47630 stimulation. As shown in Fig. 3E, TNF-α, IL-10, IL-12, and IFN-γ production were significantly inhibited by these three inhibitors, indicating that the MAPK pathway plays a critical role in rNFA47630-induced cytokine production.

Mice immunized with rNFA47630 induce a strong humoral immune response

To clarify whether the rNFA47630 protein induces a humoral immune response in mice, as shown in Fig. 4A, sera from rNFA47630- or PBS-immunized mice were collected seven days after the last immunization. The quantities between 1/100 and 1/51200 dilution for total IgG and IgG1, IgG2a, and IgG2b subclasses specific to rNFA47630 were determined by ELISAs. Then, we found that mice immunized with the rNFA47630 preparation elicited significantly higher titers of serum total IgG and IgG1, IgG2a, and IgG2b subclasses (predominantly for specific IgG1 subclasses) than PBS-immunized mice (Fig. 4B). In addition, western blot (Fig. 4C) suggested that rNFA47630 protein reacted with sera from rNFA47630-immunized mice but not from the controls, indicating that rNFA47630-immunized mice induced a strong and specific humoral immune response and drove a Th2-biased immune response.

rNFA47630 enhanced whole blood and neutrophil bacterial clearance effects

To evaluate the whole blood and neutrophil killing effect on rNFA47630-immunized mice, whole blood and bone marrow neutrophils were collected and mixed with *N. farcinica* suspensions for 2 h. Our results showed a marked reduction in *N. farcinica* survival both in whole blood (Fig. 4D) and neutrophils (Fig. 4E) from the rNFA47630-treated group.

rNFA47630 stimulation induced IFN-γ and IL-4 secretion in spleen cells.

Spleen cells in the PBS-immunized group were collected and stimulated with 2 µg/mL rNFA47630 protein in a 37 °C incubator, and the supernatants in each well were collected at 1, 2, and 3 days for determination of the levels of IFN-γ and IL-4. Our results demonstrate that IFN-γ increased over time from Day 1 and reached higher levels at Day 3. Additionally, there was an increase in IL-4 levels from Day 1 to Day 3, but no significant trend was observed over time (Fig. 4F).

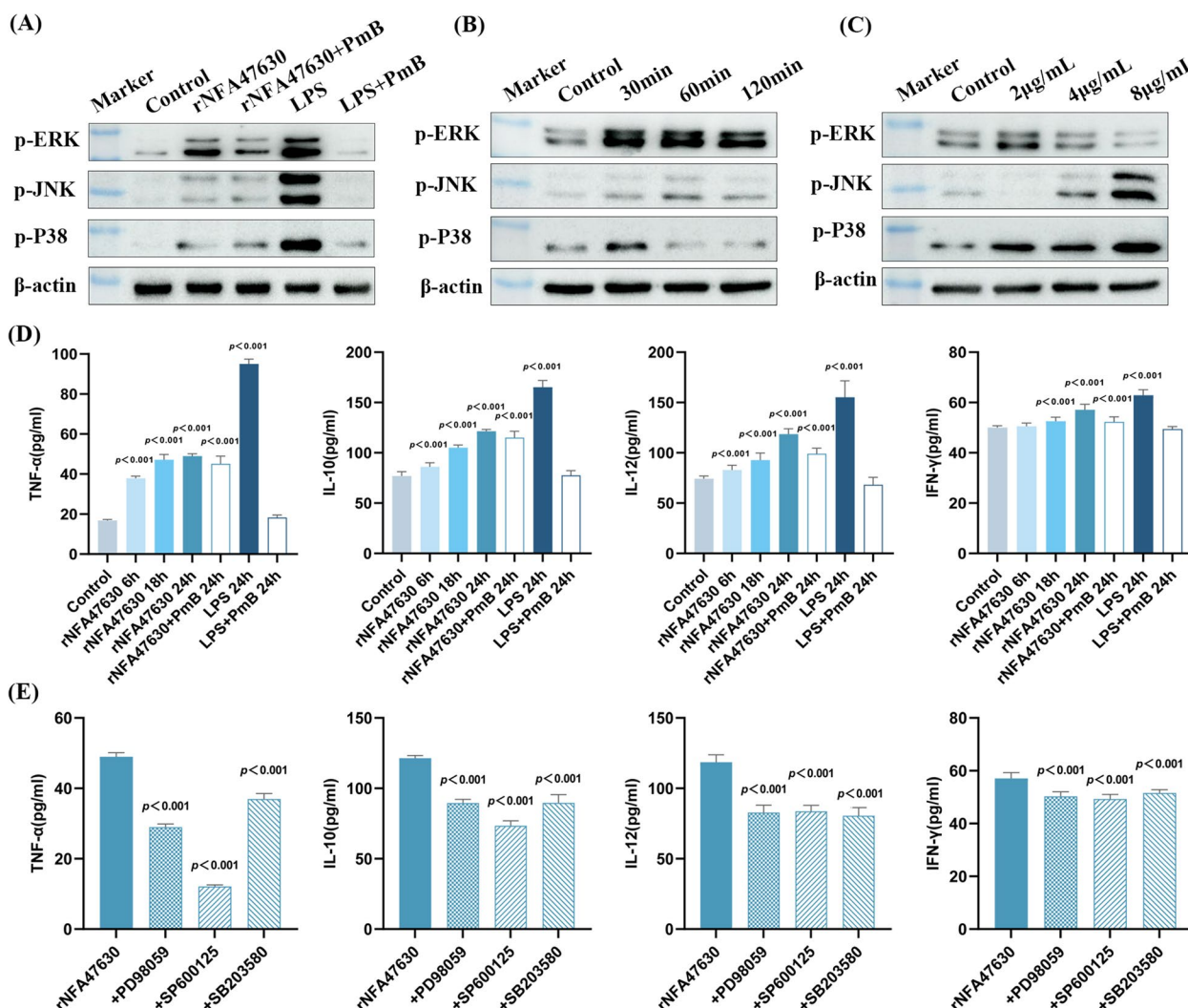


Fig. 3 rNFA47630-induced TNF- α , IL-10, IL-12, and IFN- γ secretion depended on the phosphorylation statuses of MAPK pathways. RAW264.7 cells were stimulated with 2 $\mu\text{g}/\text{mL}$ rNFA47630 (with or without PmB) or LPS (with or without PmB) for 30 min (A), or 2 $\mu\text{g}/\text{mL}$ protein for 30, 60, or 120 min (B), or 2, 4, or 8 $\mu\text{g}/\text{mL}$ protein for 30 min (C), and the phosphorylation statuses of ERK1/2, JNK and p38 were analyzed by western blot. D Cells were incubated with 2 $\mu\text{g}/\text{mL}$ rNFA47630 (with or without PmB) or LPS (with or without PmB) for 6, 18, and 24 h, and the levels of TNF- α , IL-10, IL-12, and IFN- γ in the supernatants were measured by ELISA ($n=6$ in each group). E Cells were pretreated for 1 h with inhibitors of PD 98059, SP 600125 or SB 203580 prior to rNFA47630 protein exposure, and cytokine levels were measured by ELISA ($n=6$ in each group). Data are expressed as the means \pm SDs for three independent experiments. $p < 0.001$ when compared with the control group (D) or rNFA47630 group (E)

rNFA47630 protein protects mice against challenge with *N. farcinica*.

To validate the protective effect of the rNFA47630 protein in mice, rNFA47630- and PBS-immunized mice were intranasally treated with a nonlethal *N. farcinica* suspension for 24 h. Then, we found a dramatic body temperature increase and body weight loss in the PBS-immunized group, whereas slight physical changes were observed in the rNFA47630-immunized group (Figs. 5A, B). After mice were sacrificed by cervical dislocation, alveolar lavage fluid and lung homogenate were obtained

to detect LDH levels and bacterial loads, respectively. The obtained results showed that LDH levels (Fig. 5C) and the bacterial load (Fig. 5D) of rNFA47630-immunized mice were significantly lower than those of PBS-immunized mice. Further ELISA results showed that compared with the PBS-immunized group, lower inflammatory cytokines (TNF- α , IL-10 and IL-12, Fig. 5E) and higher IFN- γ production were observed in lung supernatant from the rNFA47630-immunized group, altogether confirming that the rNFA47630 protein elicits functional immune responses in mice.

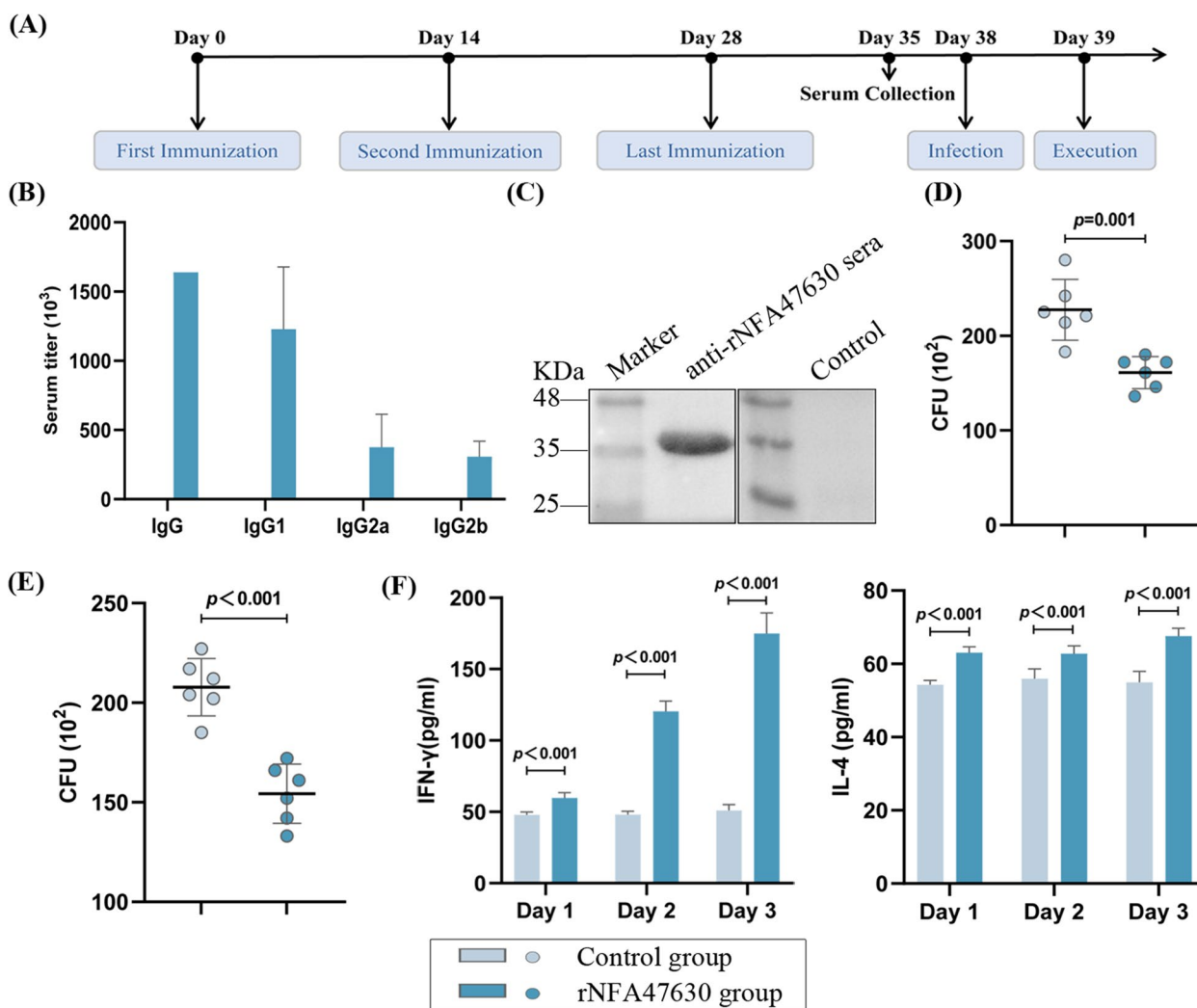


Fig. 4 Effect of rNFA47630 protein immunization in mice. **A** Female BALB/c mice were randomly divided into two groups and immunized with rNFA47630 protein or PBS three times. **B** Sera of rNFA47630-specific IgG, IgG1, IgG2a and IgG2b antibodies in PBS-immunized ($n = 6$) and rNFA47630-immunized ($n = 6$) mice were measured by ELISA. **C** Reactivity of rNFA47630 protein with anti-rNFA47630 sera. Bacterial survival in whole blood (**D**) and bone marrow neutrophils (**E**) after incubation for 2 h in control ($n = 6$) and rNFA47630 ($n = 6$) groups. **F** Spleen cells in control ($n = 6$) and rNFA47630 ($n = 6$) groups were incubated with 2 $\mu\text{g/mL}$ rNFA47630 protein for 1, 2, and 3 days, and the levels of IFN- γ and IL-4 in the supernatants were measured by ELISA. Data are expressed as the means \pm SDs for three independent experiments

Subsequently, the remaining rNFA47630- and PBS-immunized mice (10 per group) were treated with a lethal dose of *N. farcinica*, and surviving mice were counted daily for 10 consecutive days until no additional death occurred. The obtained results (Fig. 6A) showed an improved survival rate in the rNFA47630-immunized group (80%) compared with the PBS-immunized group (30%). In addition, the overall mental status of PBS-immunized mice was worse than that of rNFA47630-immunized mice. Three mice in the PBS-immunized group showed obvious neurological damage symptoms, manifested by unsteady walking. In contrast, no obvious

neurological damage was found in the rNFA47630-immunized mice.

Surviving mice in the two groups were then sacrificed by cervical dislocation at ten days postinfection. Lungs, liver and brain tissues were then dissected, fixed and stained for pathological analysis. As shown in Fig. 6B, pulmonary tissue in the PBS-immunized group showed more lymphocytes, neutrophils and macrophages infiltrated the alveolar wall (black arrows), and inflammatory cell masses were observed around the blood vessels and bronchi. In contrast, we found a small number of granulocytes infiltrating the alveolar wall (black

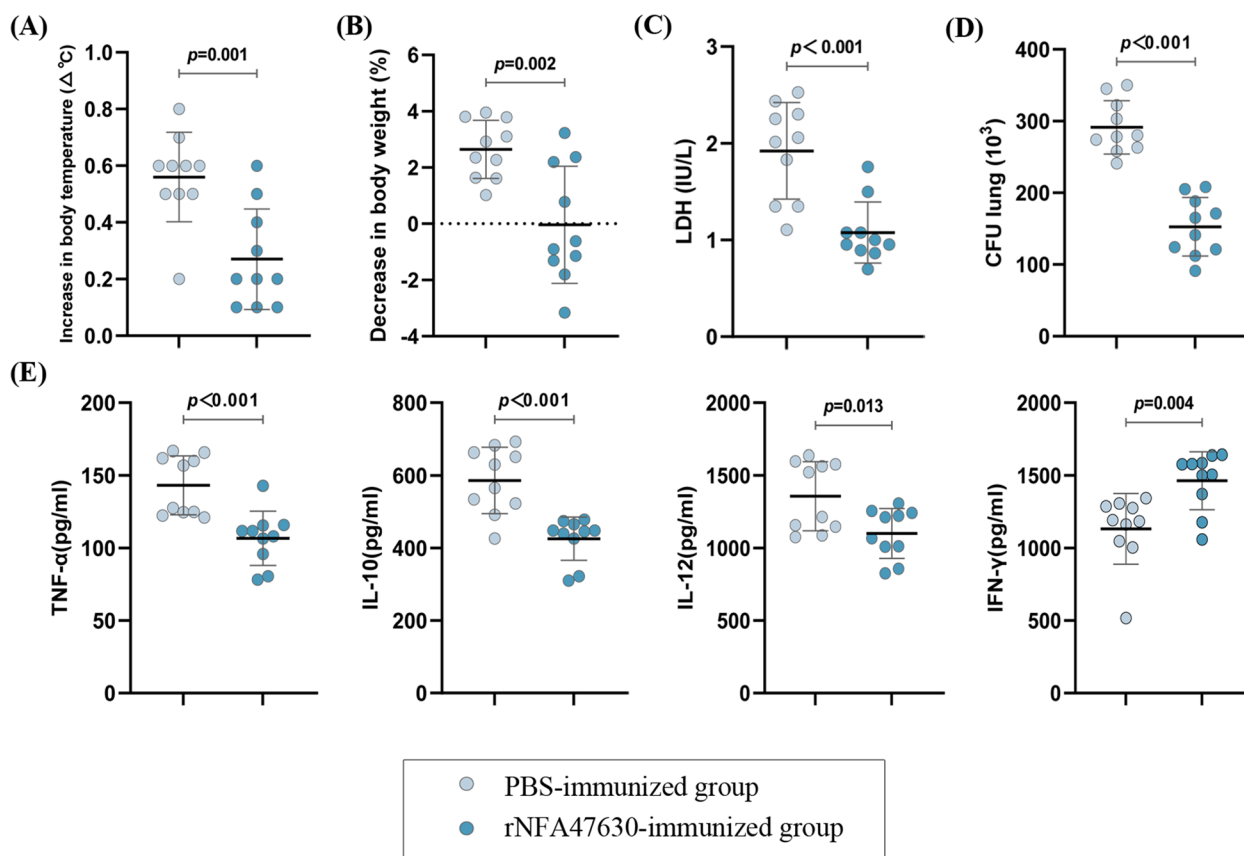


Fig. 5 rNFA47630 immunization alleviated mouse infection after challenge with *N. farcinica*. PBS-immunized ($n = 10$) and rNFA47630-immunized ($n = 10$) mice were intranasally infected with nonlethal *N. farcinica*, and then body temperature (A), body weight (B), LDH in BALF (C), CFU in lung tissue (D), and TNF- α , IL-10, IL-12, and IFN- γ in lung supernatant (E) were measured 24 h postinfection. Data are expressed as the means \pm SDs for three independent experiments

arrows) in rNFA47630-immunized mice. In addition, there were massive hepatic sinusoidal stasis and dilatation, hydropic degeneration of multiple hepatocytes (blue arrow), focal hepatocyte necrosis and nuclear lysis (yellow arrow) in the liver tissue of PBS-immunized mice. In rNFA47630-immunized mice, however, we only saw a small number of granulocytic focal infiltrates around the hepatic lobules, central veins, and confluent areas (black arrow). Furthermore, since we observed neurological symptoms in PBS-immunized mice, we performed pathological analysis of brain tissue. The results showed that more neuronal degeneration and cytoplasmic vacuolization (red arrow) in the brain tissue of PBS-immunized mice, accompanied by capillary bruising and dilatation (green arrow), whereas a small amount of neuronal degeneration (red arrow), and no obvious gliosis were observed in the rNFA47630-immunized mice. All above mentioned results indicate that immunization with the rNFA47630 protein protects mice against *N. farcinica* infections.

Discussion

As a zoonosis pathogenic bacterium, *Nocardia* can not only cause disease in human beings but also infect livestock and fish, posing increasing threats to human health and the livestock and aquaculture industries. Humans infected with *Nocardia* predominantly present with pneumonia, brain abscesses, and primary cutaneous and subcutaneous ulcers [8–11]. The clinical signs of nocardial mastitis in dairy cows included a suppurative or granulomatous inflammation of the mammary gland, reduced milk production, and no apparent clinical response to common antibiotics [27]. Infected largemouth bass *Micropterus salmoides* is characterized by hemorrhage, skin ulcers and prominent tubercles [28].

With the poor efficacy of first-line antimicrobial drugs and extensive antibiotic resistance, the development of protective antigens offers novel prevention options against *Nocardia* infections. In the aquaculture industry, vaccination against *Nocardia* infection has been developed and applied successively, including inactivated

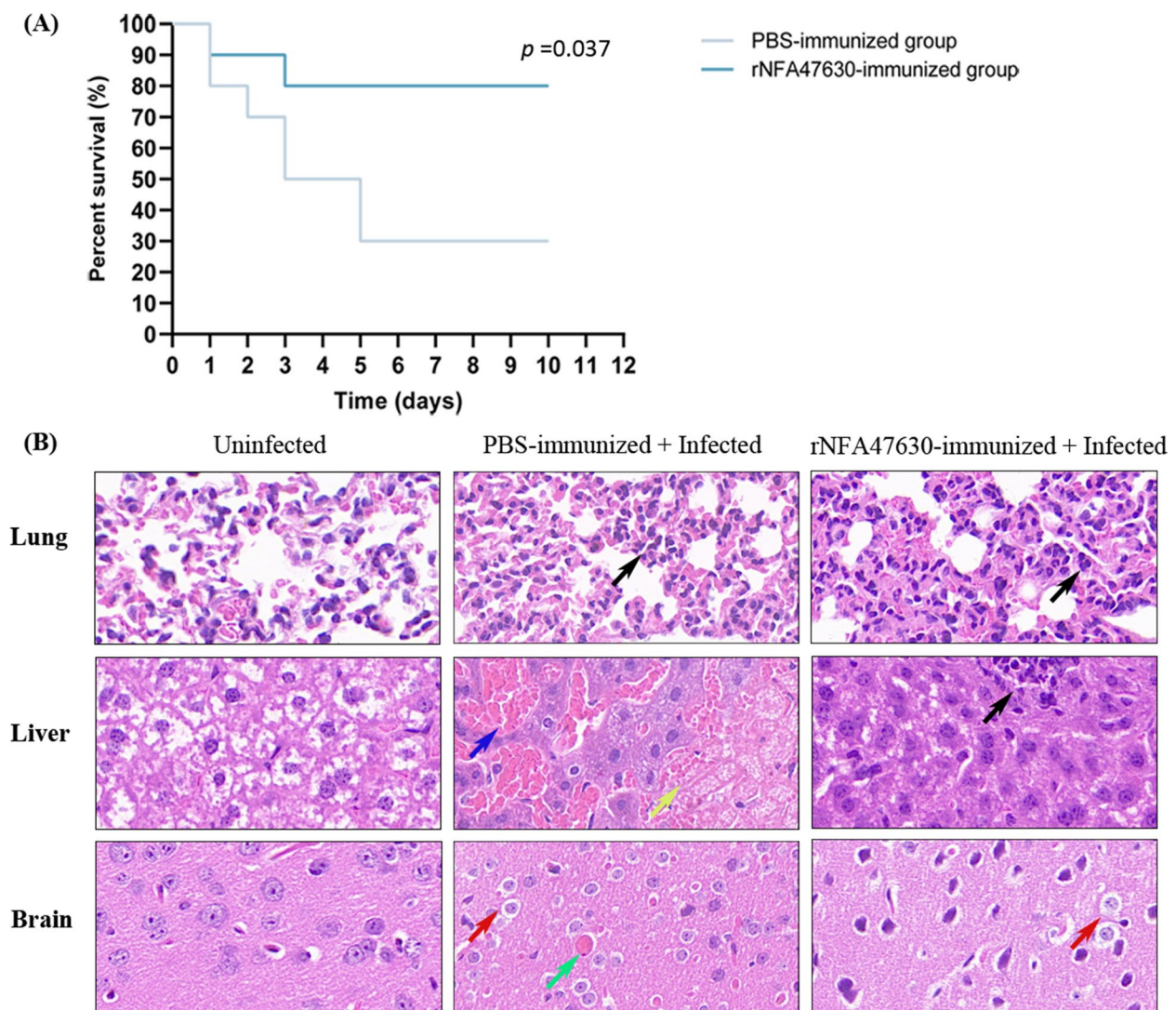


Fig. 6 rNFA47630 immunization enhanced mouse survival after challenge with *N. farcinica*. rNFA47630-immunized ($n = 10$) and PBS-immunized ($n = 10$) mice were challenged with a lethal dose of *N. farcinica* intraperitoneally, and mouse survival was monitored daily for a 10-day period **(A)**. **B** The remaining surviving mice in the two groups were sacrificed, and the lung, liver and brain **(C)** were dissected for histological examination (20 \times). Survival rates were analyzed by Kaplan–Meier and log rank test

vaccines [29], live vaccines [29], DNA vaccines [30], and subunit vaccines [31]. However, human vaccines for *Nocardia* prevention are still far from available.

Screening for immunoprotective proteins can provide effective targets for vaccine development, and many secreted proteins, such as secreted aspartyl proteinase 2 (Sap2) in *Candida* [32] and Type III secreted protein (TTSP) in *Escherichia coli* O157 [33], possess immunoprotective effects and are suitable as vaccine candidates. Previous work in our laboratory identified secreted protein NFA47630 was abundant in the supernatant of *N. farcinica* IFM10152. In this work, we first conducted conservative analysis in *N. farcinica* strains, followed

by bioinformatic analysis. The obtained results showed that *nfa47630* was conserved in *N. farcinica* strains both in model strains and clinical strains, with potential antigenicity. Then, we established a prokaryotic expression vector in *E. coli* BL21(DE3) using the pET30a plasmid. Under the optimal expression conditions of 28 °C and 0.2 mM IPTG, recombinant NFA47630 protein was expressed, purified and then confirmed by SDS-PAGE analysis. Further antigenicity analysis showed that rNFA47630 can be recognized by anti-*N. farcinica* and anti-*N. cyriacigeorgica* sera but not with others, which indicated the immune cross-reaction of rNFA47630 protein between *Nocardia* species antisera.

The role of the rNFA47630 protein in innate and adaptive immunity was then illustrated because innate immunity is the basis of adaptive immunity. Innate immunity acts first once an antigen enters the host, followed by adaptive immunity. The MAPK signaling pathways have been shown to play a key role in innate immunity to defend against *Nocardia* infection by mediating the production of pro- and anti-inflammatory cytokines [25, 26]. Subsequent experiments demonstrated that rNFA47630 stimulation promoted the secretion of TNF- α , IL-10, IL-12 and IFN- γ in RAW264.7 cells, which depended on the phosphorylation and activation of the MAPK pathway.

To further evaluate the immunoprotective efficacy of the rNFA47630 protein in mice, a conventional aluminum hydroxide adjuvant was selected and used in the immunization process considering its safety, effectiveness and wide use in clinical practice. BALB/c mice were vaccinated with PBS or rNFA47630 protein adjuvanted with aluminum hydroxide adjuvant, followed by the detection of immunogenicity. Then, we found that rNFA47630-immunized mice elicited high antigen-specific antibody titers, predominantly IgG1. Subsequently, we evaluated the effect of the rNFA47630 protein on neutrophil clearance in *Nocardia*, considering that neutrophils play a critical role during the initial phases of pulmonary nocardiosis [34]. Mouse survival from *Nocardia* infection is highly dependent on CXC chemokine receptor-2 (CXCR2) ligand-mediated neutrophil chemotaxis and subsequent bacterial clearance [34]. Our results provide preliminary evidence that immunization with rNFA47630 enhanced whole blood and neutrophil bacterial clearance effects. Subsequent experiments also showed increased secretion of IFN- γ and IL-4 in rNFA47630-stimulated spleen cells, further indicating the potential immunoprotective effect of the rNFA47630 protein.

In this work, we used two animal models to evaluate the potential immunoprotective effect of rNFA47630. First, a mouse pneumonia model mimicking the predominant infection pathways and pathogenic mechanisms of *N. farcinica* was established. Mice were administered nonlethal *N. farcinica* through intranasal inoculation. After 24 h postinfection, minor physical changes and decreased LDH, lung bacterial loads and inflammatory cytokines (TNF- α , IL-10 and IL-12) were observed in rNFA47630-immunized mice compared with PBS-immunized mice. IFN- γ plays a key role in defending against pathogen invasion that triggers multiple antimicrobial effector functions, regulating proteins that support oxidative, nitrosative, protonative, and membranolytic defense [12]. In this work, enhanced IFN- γ production was observed in rNFA47630-immunized mice, which contributed to inhibiting the intracellular growth of

Nocardia. Furthermore, mice were challenged intraperitoneally with lethal doses of *N. farcinica* suspension, and our results demonstrated increased survival in the rNFA47630-immunized group. More importantly, severe neurological symptoms (3/10) was observed in the PBS-immunized mice but not in the rNFA47630-immunized mice. Central nervous system (CNS) involvement may occur via hematogenous spread because *Nocardia* has a unique tropism for the brain, causing cerebral infiltration, meningitis, and even brain abscess. Patients with nocardial brain abscesses have high mortality rates, up to 30% [2], and the overall prognosis remains unsatisfactory. Even if the underlying infection is successfully treated, there may be residual complications such as motor impairment and hearing loss. Our results suggest that the NFA 47630 protein may have a defensive effect against CNS infections caused by *N. farcinica* strains. Further results of pathological analysis also demonstrated milder organ damage in the rNFA47630-immunized group.

Taken together, these results corroborate the notion that rNFA47630 protein immunization protects mice from *N. farcinica* infections. This provided an experimental reference for the selection of effective target antigens in follow-up clinical application. However, there are still a few potential limitations in this study. *Nocardia* typically manifest as opportunistic infections in appropriate individuals, especially in immunocompromised human. However, BALB/c female mice, the animal model used in this study, are immunocompetent hosts, the protective efficacy of rNFA47630 protein in immunocompromised hosts is still unknown. Further research on the immunoprotective effect of rNFA47630 protein requires the valuation of more influencing factors on experimental animals, such as gender, age, immune function, etc. Furthermore, the mechanism of rNFA47630 protein as a immunoprotective protein still needs further exploration. In addition, whether rNFA47630 protein can be generated for all *Nocardia* pathogen infections remains to be further verified, ongoing research in our laboratory is further valuating the immunoprotective effect of rNFA47630 protein on mice infected with isolated *N. farcinica* strains mentioned in Table S1 and other *Nocardia* species.

Conclusion

The uncharacterized NFA47630 protein from *N. farcinica* IFM10152 is a conserved protein with good antigenicity. It can not only activate innate immune signaling pathways but also induce immunoprotective effects in mice. rNFA47630-immunized mice exhibited high antigen-specific antibody titers, enhanced bacterial clearance ability, reduced organ infection, and decreased lethality, which indicated that NFA47630 was suitable as a promising vaccine candidate against a wide range of *N. farcinica* strains.

Supplementary Information

The online version contains supplementary material available at <https://doi.org/10.1186/s40794-024-00229-w>.

Supplementary Material 1.

Supplementary Material 2.

Acknowledgements

We thank American Journal Experts (AJE) for its linguistic assistance during the preparation of this manuscript.

Conflicts of interest

The authors declare that the research was conducted in the absence of any commercial or financial relationships that could be construed as a potential conflict of interest.

Code availability

Not applicable.

Authors' contributions

Lichao Han: Conceptualization, Investigation, Methodology, Writing—original draft. Xingzhao Ji, Shihong Fan: Software, Writing—review & editing. Jirao Shen, Bin Liang: Investigation, Data curation, Resources. Zhenjun Li: Supervision, Writing—review & editing, Funding acquisition. All authors contributed to the article and approved the submitted version.

Funding

This work was supported by National Key R&D Program of China (grant numbers 2021YFC2301001), the National Natural Science Foundation of China (grant number 82073624, 82102395) and Shandong Provincial Natural Science Foundation (ZR2021QH083) for the funding support.

Availability of data and materials

No datasets were generated or analysed during the current study.

Declarations

Ethics approval and consent to participate

All animal procedures were conducted in compliance with the Ethics Review Committee of the National Institute for Communicable Disease Control and Prevention at the Chinese Center for Disease Control and Prevention (2020–018). All efforts were made to minimize suffering. Not applicable.

Consent for publication

Not applicable.

Competing interests

The authors declare no competing interests.

Received: 20 February 2024 Accepted: 8 July 2024

Published online: 15 October 2024

References

- Barka EA, Vatsa P, Sanchez L, Gaveau-Vaillant N, Jacquard C, Meier-Kolthoff JP, Klenk HP, Clément C, Ouhdouch Y, van Wezel GP. Taxonomy, physiology, and natural products of *Actinobacteria*. *Microbiol Mol Biol Rev*. 2015;80(1):1–43. <https://doi.org/10.1128/MMBR.00019-15>.
- Mehta HH, Shamoo Y. Pathogenic *Nocardia*: A diverse genus of emerging pathogens or just poorly recognized? *PLoS Pathog*. 2020;16(3):e1008280. <https://doi.org/10.1371/journal.ppat.1008280>.
- Brown-Elliott BA, Brown JM, Conville PS, Wallace RJ Jr. Clinical and laboratory features of the *Nocardia* spp. based on current molecular taxonomy. *Clin Microbiol Rev*. 2006;19(2):259–82. <https://doi.org/10.1128/CMR.19.2.259-282.2006>.
- Zhang L, Yang Y, Huang S. Disseminated *Nocardia farcinica* infection in a patient with EGPA receiving immunotherapy. *Lancet Infect Dis*. 2021;21(1):148. [https://doi.org/10.1016/S1473-3099\(20\)30698-8](https://doi.org/10.1016/S1473-3099(20)30698-8).
- Clark NM, Reid GE, AST Infectious Diseases Community of Practice. *Nocardia* infections in solid organ transplantation. *Am J Transplant*. 2013;13(Suppl 4):83–92. <https://doi.org/10.1111/ajt.12102>.
- Courbin V, Riller Q, Amegnin JL, Gricourt G, Demontant V, Fihman V, Angebault C, Mahevas M, Gaube G, Coutte L, Pawlotsky JM, Lepeule R, Rodriguez C, Woerther PL. Case report: Cerebral nocardiosis caused by *Nocardia cyriacigeorgica* detected by metagenomics in an apparently immunocompetent patient. *Front Immunol*. 2022;3(13):719124. <https://doi.org/10.3389/fimmu.2022.719124>.
- Martínez-Barricarte R. Isolated Nocardiosis, an Unrecognized Primary Immunodeficiency? *Front Immunol*. 2020;20(11):590239. <https://doi.org/10.3389/fimmu.2020.590239>.
- Wilson JW. Nocardiosis: updates and clinical overview. *Mayo Clin Proc*. 2012;87(4):403–7. <https://doi.org/10.1016/j.mayocp.2011.11.016>.
- Abreu C, Rocha-Pereira N, Sarmiento A, Magro F. *Nocardia* infections among immunomodulated inflammatory bowel disease patients: A review. *World J Gastroenterol*. 2015;21(21):6491–8. <https://doi.org/10.3748/wjg.v21.i21.6491>.
- Ramos-E-Silva M, Lopes RS, Trope BM. Cutaneous nocardiosis: A great imitator. *Clin Dermatol*. 2020;38(2):152–9. <https://doi.org/10.1016/j.clindermatol.2019.10.009>.
- Corsini Campioli C, Castillo Almeida NE, O'Horo JC, Challener D, Go JR, DeSimone DC, Sohail MR. Clinical presentation, management, and outcomes of patients with brain abscess due to *Nocardia* species. *Open Forum Infect Dis*. 2021;8(4):ofab067. <https://doi.org/10.1093/ofid/ofab067>.
- Derungs T, Leo F, Loddenkemper C, Schneider T. Treatment of disseminated nocardiosis: a host-pathogen approach with adjuvant interferon gamma. *Lancet Infect Dis*. 2021;21(10):e334–40. [https://doi.org/10.1016/S1473-3099\(20\)30920-8](https://doi.org/10.1016/S1473-3099(20)30920-8).
- Khan Z, Al-Sayer H, Chugh TD, Chandy R, Provost F, Boiron P. Antimicrobial susceptibility profile of soil isolates of *Nocardia asteroides* from Kuwait. *Clin Microbiol Infect*. 2000;6(2):94–8. <https://doi.org/10.1046/j.1469-0691.2000.00026.x>.
- Larruskain J, Idigoras P, Marimón JM, Pérez-Trallero E. Susceptibility of 186 *Nocardia* sp. isolates to 20 antimicrobial agents. *Antimicrob Agents Chemother*. 2011;55(6):2995–8. <https://doi.org/10.1128/AAC.01279-10>.
- Mehta H, Weng J, Prater A, Elworth RAL, Han X, Shamoo Y. Pathogenic *Nocardia cyriacigeorgica* and *Nocardia nova* evolve to resist trimethoprim-sulfamethoxazole by both expected and unexpected pathways. *Antimicrob Agents Chemother*. 2018;62(7):e00364–e418. <https://doi.org/10.1128/AAC.00364-18>.
- Hoshino Y, Fujii S, Shinonaga H, Arai K, Saito F, Fukai T, Satoh H, Miyazaki Y, Ishikawa J. Monooxygenation of rifampicin catalyzed by the *rox* gene product of *Nocardia farcinica*: structure elucidation, gene identification and role in drug resistance. *J Antibiot (Tokyo)*. 2010;63(1):23–8. <https://doi.org/10.1038/ja.2009.116>.
- Kogure T, Shimada R, Ishikawa J, Yazawa K, Brown JM, Mikami Y, Gono T. Homozygous triplicate mutations in three 16S rRNA genes responsible for high-level aminoglycoside resistance in *Nocardia farcinica* clinical isolates from a Canada-wide bovine mastitis epizootic. *Antimicrob Agents Chemother*. 2010;54(6):2385–90. <https://doi.org/10.1128/AAC.00021-10>.
- Han L, Ji X, Yang C, Zhao S, Fan S, Zhao L, Qiu X, Yao J, Liu X, Li F, Li Z. Immunoprotective analysis of the NFA49590 protein from *Nocardia farcinica* IFM 10152 demonstrates its potential as a vaccine candidate. *Pathogens*. 2022;11(12):1488. <https://doi.org/10.3390/pathogens1121488>.
- Yu NY, Wagner JR, Laird MR, Melli G, Rey S, Lo R, Dao P, Sahinalp SC, Ester M, Foster LJ, Brinkman FS. PSORTb 30: improved protein subcellular localization prediction with refined localization subcategories and predictive capabilities for all prokaryotes. *Bioinformatics*. 2010;26(13):1608–15. <https://doi.org/10.1093/bioinformatics/btq249>.
- UniProt Consortium. UniProt: the universal protein knowledgebase in 2021. *Nucleic Acids Res*. 2021;49(D1):D480–9. <https://doi.org/10.1093/nar/gkaa1100>.
- Tusnady GE, Simon I. The HMMTOP transmembrane topology prediction server. *Bioinformatics*. 2001;17(9):849–50. <https://doi.org/10.1093/bioinformatics/17.9.849>.

22. Garcia-Boronat M, Diez-Rivero CM, Reinherz EL, Reche PA. PVS: a web server for protein sequence variability analysis tuned to facilitate conserved epitope discovery. *Nucleic Acids Res.* 2008;36(Web Server issue):W35–41. <https://doi.org/10.1093/nar/gkn211>.
23. Wang L, Zhang X, Wu G, Qi Y, Zhang J, Yang J, Wang H, Xu W. *Streptococcus pneumoniae* aminopeptidase N contributes to bacterial virulence and elicits a strong innate immune response through MAPK and PI3K/AKT signaling. *J Microbiol.* 2020;58(4):330–9. <https://doi.org/10.1007/s12275-020-9538-0>.
24. Beaman BL. In vitro response of rabbit alveolar macrophages to infection with *Nocardia asteroides*. *Infect Immun.* 1977;15(3):925–37. <https://doi.org/10.1128/iai.15.3.925-937.1977>.
25. Han L, Ji X, Xu S, Fan S, Wang C, Wei K, Wang X, Song H, Zheng N, Sun L, Qiu X, Hou X, Li Z. Microbiological profile of distinct virulence of *Nocardia cyriacigeorgica* strains in vivo and in vitro. *Microb Pathog.* 2020;8(142):104042. <https://doi.org/10.1016/j.micpath.2020.104042>.
26. Ji X, Zhang X, Li H, Sun L, Hou X, Song H, Han L, Xu S, Qiu X, Wang X, Zheng N, Li Z. Nfa34810 facilitates *Nocardia farcinica* invasion of host cells and stimulates tumor necrosis factor alpha secretion through activation of the NF- κ B and mitogen-activated protein kinase pathways via toll-like receptor 4. *Infect Immun.* 2020;88(4):e00831–e919. <https://doi.org/10.1128/IAI.00831-19>.
27. Pisoni G, Locatelli C, Alborali L, Rosignoli C, Allodi S, Riccaboni P, Grieco V, Moroni P. Short communication: outbreak of *Nocardia neocaledoniensis* mastitis in an Italian dairy herd. *J Dairy Sci.* 2008;91(1):136–9. <https://doi.org/10.3168/jds.2007-0477>.
28. Ho PY, Chen YC, Maekawa S, Hu HH, Tsai AW, Chang YF, Wang PC, Chen SC. Efficacy of recombinant protein vaccines for protection against *Nocardia seriolae* infection in the largemouth bass *Micropterus salmoides*. *Fish Shellfish Immunol.* 2018;78:35–41. <https://doi.org/10.1016/j.fsi.2018.04.024>.
29. Nayak SK, Shibasaki Y, Nakanishi T. Immune responses to live and inactivated *Nocardia seriolae* and protective effect of recombinant interferon gamma (rIFN γ) against nocardiosis in ginbuna crucian carp, *Carassius auratus langsdorffii*. *Fish Shellfish Immunol.* 2014;39(2):354–64. <https://doi.org/10.1016/j.fsi.2014.05.015>.
30. Chen J, Chen Z, Wang W, Hou S, Cai J, Xia L, Lu Y. Development of DNA vaccines encoding ribosomal proteins (RplL and RpsA) against *Nocardia seriolae* infection in fish. *Fish Shellfish Immunol.* 2020;96:201–12. <https://doi.org/10.1016/j.fsi.2019.12.014>.
31. Hoang HH, Wang PC, Chen SC. Recombinant resuscitation-promoting factor protein of *Nocardia seriolae*, a promising vaccine candidate for largemouth bass (*Micropterus salmoides*). *Fish Shellfish Immunol.* 2021;111:127–39. <https://doi.org/10.1016/j.fsi.2021.01.015>.
32. Shukla M, Rohatgi S. Vaccination with secreted aspartyl proteinase 2 protein from *Candida parapsilosis* can enhance survival of mice during *C. tropicalis*-mediated systemic candidiasis. *Infect Immun.* 2020;88(10):e00312–e320. <https://doi.org/10.1128/IAI.00312-20>.
33. Allen KJ, Rogan D, Finlay BB, Potter AA, Asper DJ. Vaccination with type III secreted proteins leads to decreased shedding in calves after experimental infection with *Escherichia coli* O157. *Can J Vet Res.* 2011;75(2):98–105.
34. Moore TA, Newstead MW, Strieter RM, Mehrad B, Beaman BL, Standiford TJ. Bacterial clearance and survival are dependent on CXC chemokine receptor-2 ligands in a murine model of pulmonary *Nocardia asteroides* infection. *J Immunol.* 2000;164(2):908–15. <https://doi.org/10.4049/jimmunol.164.2.908>.

Publisher's Note

Springer Nature remains neutral with regard to jurisdictional claims in published maps and institutional affiliations.